Expression and Localization of Tenomodulin, a Transmembrane Type Chondromodulin-I–Related Angiogenesis Inhibitor, in Mouse Eyes

Yusuke Oshima,[1,2] *Chisa Shukunami,*[2] *Junichi Honda,*[2] *Koji Nishida,*[1] *Fumi Tashiro,*[3] *Jun-ichi Miyazaki,*[3] *Yuji Hiraki,*[2] *and Yasuo Tano*[1]

Purpose. To explore the role in the eye of tenomodulin (TeM), a chondromodulin (ChM)-I–related glycoprotein, the expression, localization, and antiangiogenic potential of TeM were investigated.

Methods. Gene expression and protein localization of TeM in mouse eyes were examined by Northern blot analysis, in situ hybridization, and immunohistochemical analysis. Antiangiogenic function included in the C terminus of TeM and ChM-I was examined in vascular endothelial cells through adenoviral gene transduction.

Results. TeM expression was detectable from day 15 of the embryonic stage and was clearly present in the eye and skin. In situ hybridization of the eye tissues revealed TeM mRNA in the tendon of the extraocular muscle, the sclerocornea, the lens fiber cells, and the ganglion cell layer, inner nuclear layer cells, and pigment epithelium of the retina. Corresponding immunoreactivity of TeM was present in most of these cells. Western blot detected 40- and 45-kDa immunoreactive bands of TeM in the eye as differently glycosylated forms of the transmembrane protein. Production of a secreted form of TeM and ChM-I through adenoviral gene transfer caused effective autocrine suppression of cell proliferation and capillary-like morphogenesis of retina vascular endothelial cells. The condition media from soluble TeM- and ChM-I–overexpressing cells also showed a marked inhibitory effect on in vitro angiogenesis.

Conclusions. These results indicate a potential role for TeM in prevention of vascular invasion in the mouse eye and the possibility of both TeM and ChM-I as candidates for use in gene therapy approaches to treatment of ocular angiogenesis. (*Invest Ophthalmol Vis Sci.* 2003;44:1814–1823) DOI:10.1167/iovs.02-0664

From the [1]Department of Ophthalmology and Visual Science, Osaka University Medical School, Osaka, Japan; the [2]Department of Molecular Interaction and Tissue Engineering, Institute for Frontier Medical Sciences, Kyoto University, Kyoto, Japan; and the [3]Department of Nutrition and Physiological Chemistry, Osaka University Graduate School of Medicine, Osaka, Japan.

Supported in part by the Japan Society for the Production of Science Research for the Future Program (YH) and grants-in-aid from the Ministry of Education, Culture, Sports, Science, and Technology of Japan (YH, CS, YT).

Submitted for publication July 3, 2002; revised September 25 and November 5, 2002; accepted November 26, 2002.

Disclosure: **Y. Oshima**, None; **C. Shukunami**, None; **J. Honda**, None; **K. Nishida**, None; **F. Tashiro**, None; **J.-I. Miyazaki**, None; **Y. Hiraki**, None; **Y. Tano**, None

The publication costs of this article were defrayed in part by page charge payment. This article must therefore be marked "*advertisement*" in accordance with 18 U.S.C. §1734 solely to indicate this fact.

Corresponding author: Yusuke Oshima, Department of Ophthalmology and Visual Science, Osaka University Medical School, 2-2 Yamadaoka, Rm. E7, Suita, Osaka 565-0871, Japan; oshima@ophthal.med.osaka-u.ac.jp.

Ocular angiogenesis, the pathologic growth of new blood vessels in the eye, is a leading cause of blindness worldwide. Neovascularization is responsible for many severe ocular disorders, such as corneal conjunctivalization, neovascular glaucoma, diabetic retinopathy, age-related macular degeneration, and retinopathy of prematurity.[1,2] The control of ocular neovascularization would be promising for the treatment of these disorders. Similar to the well-known angiogenic mechanism in tumor growth, neovascularization in the eye is also considered to result from an imbalance between stimulatory and inhibitory angiogenic factors.[3,4] The elevated expression of stimulatory factors and/or the downregulation of inhibitory factors is often observed in pathologic conditions such as ocular inflammation and ischemia.[5–8] In contrast to these pathologic conditions, ocular tissues are maintained physiologically without the occurrence of neovascularization, and vasculature in the eye is highly restricted despite the presence of many angiogenesis-stimulating molecules in the eye, such as basic fibroblast growth factor (bFGF),[9,10] insulin-like growth factor (IGF)-1,[11] and vascular endothelial growth factor (VEGF).[12,13] These findings suggest the physiological existence in the eye of angiogenesis inhibitors to counterbalance these stimulators. Potent inhibitory factors have been thought to exist in the retinal pigment epithelium (RPE),[14] the vitreous body,[15–19] and the lens,[20] although most of them have not been isolated yet. Up to date, pigment epithelium-derived factor (PEDF), a neurotrophic factor and a member of the serine protease inhibitor superfamily, has been identified as a major angiogenesis inhibitor in the eye.[21–23] Recently, we demonstrated that chondromodulin (ChM)-I, a ~25-kDa glycoprotein purified as a cartilage-derived chondrocyte growth factor,[24] is another angiogenesis inhibitor specifically expressed not only in the cartilaginous tissues but also in the eye.[25–28] ChM-I is expressed in the ciliary body, the ganglion cell layer of the retina, and the RPE,[27,28] and suppresses proliferation and capillary formation of retinal vascular endothelial cells in vitro and angiogenesis in vivo.[25,28–30]

Recently, three independent groups reported the identification of a novel gene, tenomodulin (TeM; also referred to as ChM-IL or tendin), which is homologous to ChM-I.[31–33] TeM is a glycoprotein with significant amino acid sequence homology (36%) with the ChM-I precursor.[31,32] Cloning of the full-length cDNA of TeM revealed that the TeM protein (317 amino acid residues) has a single transmembrane domain in the N-terminal region, two N-linked glycosylation sites, and a cysteine-rich domain (Phe^{225}-Val^{317}) in the C-terminal region.[31–33] TeM and ChM-I exhibit the strongest sequence identity (65%) within the C-terminal 63-amino-acid stretch, which corresponds to the predicted antiangiogenic functional domain of ChM-I (Phe^{272}-Val^{334}).[32] Both TeM and ChM-I carry eight cysteine residues in their C-terminal domains, and the spacing of the eight cysteine residues in TeM is almost identical with that in ChM-I.[31,32] However, in contrast to ChM-I, the mature form of which is a secreted protein existing in the extracellular matrix after being processed from the transmembrane-type precursor,[24] TeM is a

Investigative Ophthalmology & Visual Science, May 2003, Vol. 44, No. 5

transmembrane protein presumably located at the cell surface, because it lacks the hormone-processing signal present in the ChM-I precursor.[31,32] TeM mRNA has been demonstrated to be specifically expressed in hypovascular connective tissues such as the tendon and ligament.[32,33] Because of the similarity in the C-terminal characteristics between TeM and ChM-I and the structural analogy noted between skeletal connective tissues and the eye in hypovascularity and components of the extracellular matrix, it can be speculated that TeM also participates in maintenance of the avascular condition in the eye.

In the present study, we investigated the gene expression of TeM in the eye by Northern blot analysis and in situ hybridization and the localization of its protein by Western blot and immunohistochemical analysis. To elucidate the antiangiogenic potential included in the C terminus of TeM and ChM-I, soluble TeM and ChM-I were produced through adenoviral gene transduction into human vascular endothelial cells, and angiogenesis assays were conducted in cell cultures.

Materials and Methods

Tissues Preparation and Cell Culture

All experiments were conducted in accordance with the Animal Care and Use Committee guidelines and the ARVO Statement for the Use of Animals in Ophthalmic and Vision Research. DDY mice, an albino mouse strain with no pigmentation in the RPE, were anesthetized with diethyl ether and killed by cutting the axillary artery. Systemic organs (eye, liver, skin, and thymus) were removed from 4-week-old mice. Embryos were collected at postcoital days 12.5 and 16.5.

Human retinal vascular endothelial cells (HRECs) and human umbilical vein endothelial cells (HUVECs) were purchased from Applied Cell Biology Research Institute (Kirkland, WA) and grown in complete medium with supplements (EGM2; Clonetics, Walkersville, MD). Cells at passages 3 through 6 were used for the experiments. Within these passages, both HRECs and HUVECs maintained their endothelial characteristics, such as the cobblestone-like morphogenesis, Ac-LDL uptake and the tubelike morphogenesis on collagen gel and expressed vascular endothelium-specific marker such as platelet–endothelial cell adhesion molecule (PECAM; CD31) on the cell surfaces. The 293 cell line, a human embryonic kidney cell line constitutively producing the adenovirus E1 protein,[34] was purchased from the American Type Culture Collection, Manassas, VA) and cultured in Dulbecco's modified Eagle's medium (DMEM) containing 10% fetal bovine serum (FBS).

Northern Blot Analysis

Total cellular RNA was purified from organs of 4-week-old mice by a modified acid guanidium thiocyanate phenol-chloroform extraction method.[35] Total RNA (20 μg) was denatured and transferred onto membranes (Nytran; Schleicher & Schuell, Dassel, Germany). A Northern blot containing 2 μg of poly(A)$^+$ RNA isolated from mouse embryos at different developmental stages was used (Clontech Laboratories Inc., Palo Alto, CA). Hybridization of the blots was performed at 42°C overnight with radiolabeled probes, using the appropriate cDNA fragments, as previously described: a 460-bp *Eco*RI fragment as a probe for TeM and a 1.3-kb *Eco*RI fragment as a probe for ChM-I.[32,36] After hybridization, the membrane filter was washed at 55°C at high stringency and exposed to autoradiographic film (Biomax; Eastman Kodak, Rochester, NY) at −80°C.

RT-PCR Analysis

Total RNA was purified from eye tissues of 4-week-old mice and reverse transcribed (Superscript Pre-amplification System; Gibco BRL, Grand Island, NY).[31,35] The cDNAs were amplified for 25 cycles (30 seconds at 94°C, 45 seconds at 58°C, and 60 seconds at 72°C) using mouse TeM-specific primers (forward primer: 5′-GAA ACC ATG GCA AAG AAT CCT CCA GAG-3′; reverse primer: 5′-TTA GAC TCT CCC AAG CAT GCG GGC-3′). Glyceraldehyde-3-phosphate dehydrogenase (G3PDH)–specific primers (forward primer: 5′-TCC TGC ACC ACC AAC TGC TTA GC-3′; reverse primer: 5′-TTA CTC CTT GGA GGC CAT-3′) were used as a positive control. PCR products were electrophoresed and visualized by ethidium bromide staining.

In Situ Hybridization

Embryos at postcoital day 16.5 and tissues from 4-week-old mice were fixed with 4% paraformaldehyde in 0.1 M phosphate buffer (PB) overnight, embedded in paraffin, and sectioned at a thickness of 6 μm. In situ hybridization was performed as previously described.[32] In brief, a 1.0-kb fragment of mouse TeM or ChM-I cDNA subcloned into a vector (pCRII TA; Invitrogen, San Diego, CA) was used as a template for in vitro transcription after linearization of the plasmid. Digoxigenin (DIG)-labeled antisense and sense riboprobes were prepared with a DIG RNA labeling kit (Roche Molecular Biochemicals, Gaithersburg, MD). After dewaxing and rehydration, hybridization was performed at 50°C for 16 hours, and the sections were washed under conditions of high stringency. Hybridization signals were detected immunohistochemically by an alkaline phosphatase–conjugated antibody, according to the supplied instructions. The alkaline phosphatase substrate (5-bromo-a-chloro-3-indolyl phosphate/nitroblue tetrazolium [BCIP/NBT]) was used for color detection. Sections were counterstained with purified methyl green (Laboratory Vision Co., Fremont, CA), mounted on coverslips, and photographed.

Immunohistochemistry

Both frozen and paraffin-embedded tissues of embryos at postcoital day 16.5 were prepared. For frozen sections, tissues were fixed with 4% paraformaldehyde in 0.1 M PB for 4 hours followed by immersion in 25% sucrose in PBS overnight. The tissues were embedded in optimal temperature cutting compound (Tissue-Tek; Miles, Elkhart, IN), frozen in liquid nitrogen, and sectioned at 6 μm with a cryostat at −20°C. Paraffin sections were deparaffinized in xylene and treated with 1% hydrogen peroxide in methanol for 30 minutes to minimize endogenous peroxidase activity. Frozen sections were also treated with 1% hydrogen peroxide in methanol for 30 minutes to minimize endogenous peroxidase activity. Affinity-purified rabbit polyclonal anti-TeM antibody was raised against a synthetic polypeptide corresponding to amino acids 245-252 of mouse and human TeM (a kind gift from Hitoshi Wada, Teijin Institute for Biochemical Research, Teijin, Ltd. Tokyo, Japan).[32] After a wash in PBS, the sections were incubated with 0.5% normal goat serum and 1% BSA in PBS and then with the affinity-purified rabbit polyclonal anti-TeM antibody at 4°C overnight. For the control, normal rabbit IgG (Santa Cruz Biotechnology, Santa Cruz, CA) was used as the primary antibody. Immunoreactions were performed with an avidin-biotin complex (ABC) kit (Vectastain Elite; Vector Laboratories, Burlingame, CA). Sections were washed with PBS, and antigenic sites were demonstrated by treating the sections with 0.05% 3,3′-diaminobenzidine tetrahydrochloride (Dojin Chemicals, Tokyo, Japan) in 0.05 M Tris-HCl buffer (pH 7.6), and 0.01% H_2O_2. Sections were counterstained with the purified methyl green (Laboratory Vision Co.), mounted on coverslips, and photographed.

Western Blot Analysis

For detection of the natural form of TeM, mouse tissue extracts (whole eye and liver) were homogenized in homogenizing buffer (8 M urea, 50 mM Tris-HCl [pH 8.0], 1 mM dithiothreitol, and 1 mM EDTA) and centrifuged to remove the cellular debris. Aliquots (~200 μg of total protein) of the supernatants were diluted in 2× SDS sample buffer (100 mM Tris-HCl, pH 6.8), 4% SDS, 10% β-mercaptoethanol, and 20% glycerol), separated on a 12.5% gel by SDS-polyacrylamide gel electrophoresis, and transferred to a polyvinylidene difluoride membrane. The membrane was preincubated with blocking buffer and probed with the polyclonal anti-TeM antibody at 4°C overnight. After a wash with PBS, the membrane was incubated with horseradish peroxidase (HRP)–conjugated anti-rabbit IgG antibody (Amersham Pharmacia Bio-

tech, Piscataway, NJ). Protein was visualized by the enhanced chemiluminescence system (ECL Plus; Amersham Pharmacia Biotech) according to the supplied instructions.

For detection of the recombinant protein expressed in the conditioned medium, HRECs, with or without adenoviral transduction, were plated on gelatin-coated culture plates (Costar; Corning, Inc., Corning, NY) and incubated for 48 hours. The culture medium was then harvested and eluted through a separation column (butyl-Toyoperl; Tosoh Co., Tokyo, Japan). After evaporation and dilution in SDS sample buffer, Western blot was performed as described earlier. The membrane was probed with an anti-FLAG monoclonal antibody (Sigma-Aldrich, St. Louis, MO), followed by an HRP-conjugated anti-mouse IgG antibody (Amersham Pharmacia Biotech). The peroxidase activity was visualized by enhanced chemiluminescence (Amersham Pharmacia Biotech).

Expression Cassette Construction

Before preparation of the recombinant adenoviral vector, an expression cassette for generating an FLAG-tagged secreted form of the recombinant protein containing residues Glu^{202}-Val^{317} of human TeM, corresponding to the residues Glu^{215}-Val^{334} of the mature form of human ChM-I, was constructed. In brief, a cDNA fragment encoding the secretion signal of preprotrypsin and the FLAG epitope from pFLAG-CMV1 (Sigma-Aldrich) was constructed in an expression plasmid. The plasmid was flanked by the *Swa*I site and contained the strong CAG (cytomegalovirus immediate-early enhancer-chicken β-actin hybrid) promoter, an internal ribosome entry site (IRES) followed by enhanced green fluorescence protein (EGFP), and a polyadenylation signal of the rabbit β-globin gene.[37] Then, the cDNA fragment encoding residues Glu^{202}-Val^{317} of human TeM generated by PCR (forward primer: 5′-GAG GGA GAA GAT CTT CAC TTT CC-3′; reverse primer: 5′-AAT TAA CCC TCA CTA AAG GG-3′) was cloned into the plasmid to create a CAG promoter/FLAG-humanTeM(Glu^{202}-Val^{317})/IRES-EGFP expression cassette. Thus, a secreted form of TeM including the predicted functional domain of TeM was constructed. For comparison, a cDNA fragment encoding the mature form of human ChM-I was generated (forward primer: 5′-GAA GTG GTA AGA AAA ATT GTT CC-3′; reverse primer: 5′-GCG CGG CCG CTC ACT CCA TGC CCA AGA TAC GGG C-3′) and cloned into the expression plasmid described above to also create a CAG promoter/FLAG-humanChM-I(Glu^{215}-Val^{334})/IRES-EGFP expression cassette. The FLAG-tagged secreted form TeM (f-sTeM) and the FLAG-tagged mature form ChM-I (f-mChM-I) expression cassettes were excised by digestion with *Swa*I and ligated with the E1-defective adenoviral genome containing cosmid vector (pALC3.0), respectively. For introduction of the cosmids into *Escherichia coli*, an in vitro λ phage packaging kit (Stratagene, La Jolla, CA) was used according to the supplied instructions. The structure of the resultant cosmid vectors is illustrated later. An empty vector without the insertion but able to generate the EGFP protein through the IRES was used as the mock control in the present study.

Adenovirus Production

The method for the replication-defective E1-recombinant adenoviral vector preparation has been described previously.[38] To generate infectious recombinant adenoviral vectors, 1 μg of the indicated expression cosmid and 0.1 μg of pMC1-Cre for the expression of Cre recombinase were cotransfected into 293 cells, with transfection reagent (Lipofectamine 2000; GibcoBRL) used according to the supplied instructions. Cytopathic effect (CPE) in the cotransfected 293 cells was visible within 10 days. Culture media with CPE was harvested and centrifuged to obtain the supernatant fraction, which contained the adenoviral vector. After addition of the supernatant to 293 cells grown at a large scale and cultured for a further several days, 293 cells with complete CPE were harvested, lysed by six cycles of freezing and thawing, and centrifuged at 3500 rpm for 10 minutes at 4°C. The supernatant fraction, which contained the adenoviral vector, was used for evaluation of the efficiency of adenoviral vector generation and transfection according to the standard procedure described previously.[39] Manipulations of adenoviral vectors were performed in accordance with both institutional and national biosafety restrictions. For the prevention of adenovirus-induced cytotoxicity, the titer was determined that could cause apoptotic cell death within 6 to 8 passages in the cells infected with the mock vector.

Dil-Ac-LDL Uptake

To confirm the maintenance of vascular endothelial characteristics after adenoviral transduction, an Ac-LDL uptake assay was performed in the untransfected HRECs (wild type) and in the HRECs infected with the indicated adenoviral vectors. Cells were incubated with 10 μg/mL Dil-Ac-LDL (Molecular Probes, Leiden, The Netherlands) in complete medium (EGM2; Clonetics) for 6 hours and further incubated with 10 nM Hoechst 33342 (Sigma-Aldrich) for 2 hours. Dil-Ac-LDL uptake in living cells was examined and photographed and the images merged with a fluorescence microscope coupled to an imaging computer system (Carl Zeiss, Oberkochen, Germany).

HREC Proliferation

DNA synthesis measured by 5′-bromo-2′-deoxyuridine (BrdU) incorporation was performed as an index of cell proliferation. Gene-transfected or wild-type early-passage (passages 3–6) HRECs were harvested with trypsin/EDTA and suspended in medium (EGM2; Clonetics) at a density of 50,000 cells/mL. The cells were seeded in a 96-well gelatin-coated plate (100 μL per well) and grown to subconfluence. The cells were then starved in 0.5% FBS-containing DMEM for 6 hours and stimulated with VEGF (R&D Systems, Minneapolis, MN) at the indicated concentration for another 12 hours. After the stimulation, 10 μL 10× BrdU was added to each well, and the cells were further incubated for 4 hours. BrdU ELISA chemiluminescence was analyzed according to the manufacturer's protocol (Roche Molecular Biochemicals).

To investigate the bioactivity of f-sTeM and f-mChM-I in the conditioned media from HRECs, HUVECs were grown to subconfluence in a 96-well culture plate, and starved in 0.5% FBS-containing αMEM for 6 hours. The conditioned media obtained from the wild-type HRECs or the HRECs with the indicated adenoviral gene transduction were harvested from 3-day cultures and mixed with fresh DMEM at a ratio of 1:1, to contain final concentrations of 30 ng/mL VEGF. The mixed medium was used for incubation of the serum-starved HUVECs for 12 hours, and DNA synthesis was evaluated by BrdU incorporation, according to the manufacturer's protocol (Roche Molecular Biochemicals).

In Vitro Angiogenesis Assay

For the capillary-like formation assay, growth factor-reduced synthetic matrix (Matrigel; BD Labware, Bedford, MA) was applied to a 24-well tissue culture plate (400 μL per well). After a 30-minute polymerization of the matrix at 37°C, HRECs that had been serum-starved for 4 hours were harvested by using trypsin/EDTA and suspended in culture medium for 20 minutes. Cells were resuspended in migration buffer (αMEM/0.1% BSA) and finally seeded at a density of 10,000 cells per well (final volume, 500 μL) on polymerized matrix (Matrigel; BD Labware) in the presence of VEGF (10 ng/mL). The plate was incubated at 37°C for 6 hours and then photographed. For quantitative evaluation of the capillary-like morphogenesis of HRECs, four fields per well were automatically and randomly selected for digital photography, based on the computer program, and the identity of the contents of wells was masked during photography and analysis. The total length of tubelike structures per field was measured on computer with an image-processing and -analysis program (NIH image version 1.61, available by ftp from zippy.nimh.nih.gov/or from http://rsb.info.nih.gov/nih-image; developed by Wayne Rasband, National Institutes of Health, Bethesda, MD). Each experiment was performed three times, and the data were analyzed statistically with one-way analysis of variance (ANOVA), followed by the Scheffé multicomparison test.

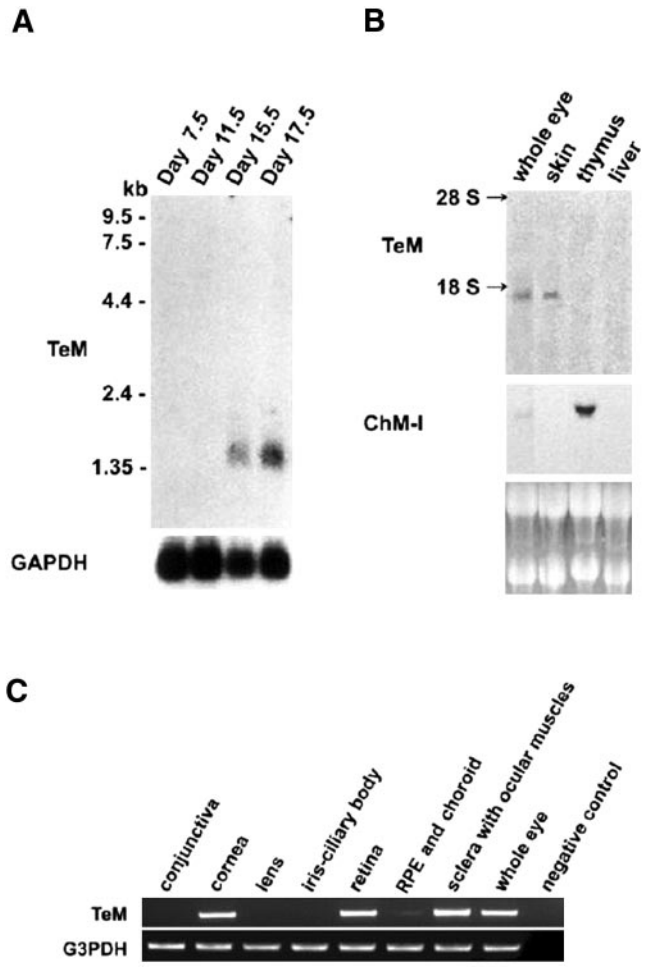

FIGURE 1. TeM mRNA expression during mouse embryonic development and tissue distribution. (**A**) Northern blot containing RNA isolated from postcoital day-7.5, -11.5, -15.5, and -17.5 mouse embryos was obtained, and hybridization analysis was performed with a radiolabeled TeM probe. *Left*: RNA size markers. (**B**) Total RNA (20 μg) was prepared from the indicated tissues of 4-week-old mice, and the same filter was sequentially hybridized with cDNA probes specific for TeM and ChM-I. The equivalent loading of each RNA was verified with ethidium bromide staining. The positions of the 28S and 18S ribosomal RNAs are indicated. (**C**) RT-PCR of the indicated eye tissues of 4-week-old mice was performed with primers specific for mouse TeM and for G3PDH.

To investigate the bioactivity of f-sTeM and f-mChM-I in the conditioned media from HRECs, a commercially available in vitro angiogenesis assay kit comprising cocultures of HUVECs and human dermal fibroblasts was purchased from TCS Biologicals (Buckinghamshire, UK) and used according to the supplied instructions.[40] The conditioned media from the wild-type HRECs or the HRECs with the indicated adenoviral gene transduction were harvested from the 3-day cultures and mixed with fresh DMEM at a ratio of 1:1 to obtain final concentrations of 10% FBS and 10 ng/mL VEGF. The mixed medium was used for incubation of the cocultures for 11 days. The cells were then fixed with 70% ethanol and incubated with diluted anti-human PECAM (CD31) antibody (Kurabo Inc., Osaka, Japan) for 1 hour followed by a 1-hour incubation with an alkaline phosphatase–conjugated secondary antibody. Visualization of the capillary structures formed by HUVECs was achieved with BCIP/NBT, and the total length of the capillary structures per field was measured and analyzed as described earlier.

RESULTS

Expression of TeM mRNA and TeM Protein

The pattern of TeM mRNA expression during mouse development was investigated with a blot containing RNA isolated from four different developmental time points. Northern hybridization analysis showed that the 1.4-kb transcripts for TeM were expressed at postcoital days 15 and 17 but were undetectable on or before day 11 (Fig. 1A). Therefore, embryos at day 16.5 were collected and sectioned for in situ hybridization to identify the precise sites for TeM mRNA expression at the embryonic stage. Tissue distribution of TeM transcripts in 4-week-old mice was also evaluated by Northern blot analysis (Fig. 1B). TeM mRNA was detected in whole eye and skin, but was detectable neither in the thymus, where ChM-I was abundantly expressed, nor in the liver. To further investigate the distribution of TeM mRNA in mouse eyes, RT-PCR was conducted and revealed that TeM mRNA was significantly expressed in the cornea, the sensory retina, and the sclera involving the ocular muscles and faintly expressed in the choroidal tissues, including the RPE (Fig. 1C).

Western blot analysis showed that the endogenous TeM proteins were detected as double bands of 40 and 45 kDa in tissue extracts from whole eyes but were undetectable in extracts from liver (Fig. 2). TeM proteins were also undetectable in the tissue extracts from thymus (data not shown).

In Situ Hybridization and Immunohistochemistry

In the horizontal sections through the optic stalk of the eyeball of a day-16.5 embryo (Fig. 3A), TeM mRNA expression was detected in the tendon of extraocular muscle, the sclera (Fig. 3B), the lens epithelial cells at the equator, and the early-differentiating secondary lens fiber cells (Fig. 3C). In contrast, no apparent hybridization signals were found in the lens when hybridized with the sense probe (Fig. 3F). TeM protein was most abundant in the differentiated secondary lens fibers (Fig. 3D) just adjacent to lens fiber cells that expressed TeM mRNA.

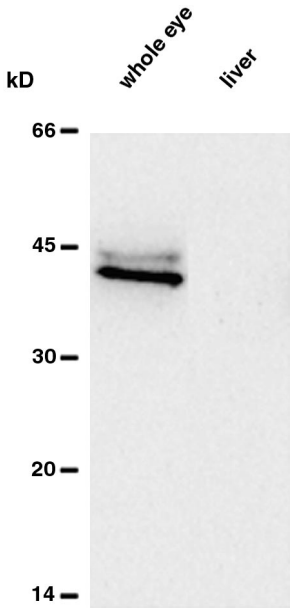

FIGURE 2. Expression of TeM protein in the mouse eye. Mouse tissue extracts were prepared from the eye and liver of 4-week-old mice. The immunoreactive double bands with a molecular mass of ~40 kDa and ~45 kDa were detectable only in extracts of the eye and were undetectable in that of the liver.

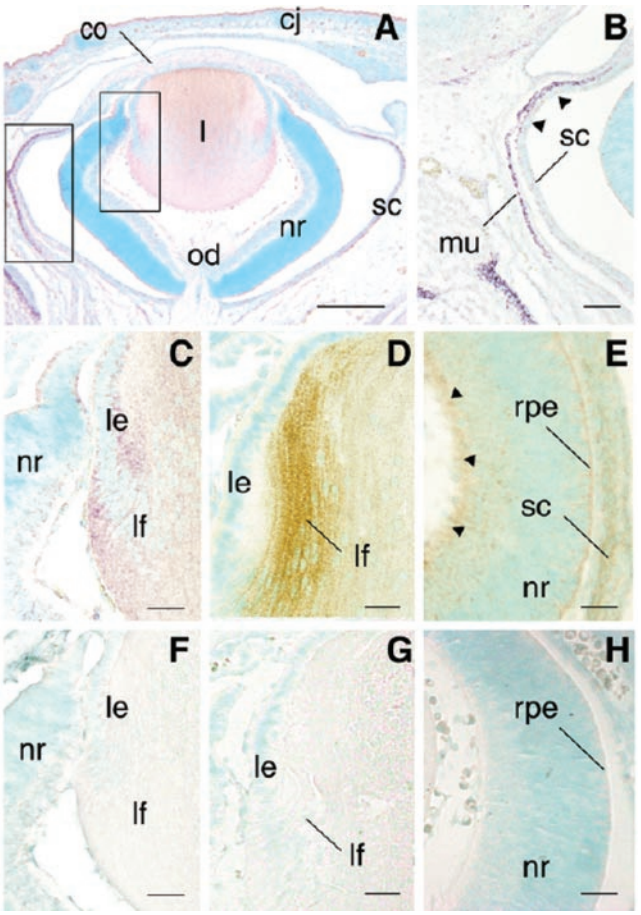

FIGURE 3. Expression of TeM mRNA and TeM protein in eye of mouse embryos. In a section of the developing eye in the day-16.5 embryos, the *boxed areas* with significant hybridization signals (*blue-violet*) in (**A**) are shown at higher magnification in (**B**) and (**C**). TeM mRNA was expressed in the developing tendon of extrinsic ocular muscle (**B**), the sclera (B; *arrowheads*), the equatorial lens epithelial cells (**C**), and the early-differentiating lens fiber cells. Strong immunoreactivity (*yellow-orange*) was found in the differentiated secondary lens fiber (**D**). In the developing retina, TeM protein was localized to the sclera (**E**), RPE (**E**), and the inner neural retina (**E**; *arrowheads*). In situ hybridization of a semiserial section hybridized with the sense probe showed no signals in the lens (**F**). No immunostaining was observed when rabbit IgG was used as the primary antibody (**G**, **H**). The sections were counterstained with methyl green. cj, conjunctiva; co, cornea; l, lens; mu, developing tendon of extraocular muscles; nr, neural retina; od, optic disc; sc, sclera; eo, extrinsic ocular muscle; le, lens epithelium; lf, lens fiber cells; rpe, RPE. Scale bars: (**A**) 350 μm; (**B**–**H**) 250 μm.

In the early-developing retina, TeM protein was detected in RPE and the inner neural retina (Fig. 3E). No immunostaining was observed when semiserial sections were incubated with normal rabbit IgG (Figs. 3G, 3H).

Analyses of TeM expression and localization in 4-week-old mice were also conducted. In situ hybridization revealed TeM mRNA expression in the stromal layer of the cornea and the sclera, and faint but significant expression in the ganglion cell layer of the retina and the inner nuclear layer cells (Figs. 4A, 4C, 4E). No apparent hybridization was found in these sites when hybridized with the sense probe (Figs. 4B, 4D, 4F).

Construction of f-sTeM– and f-mChM-I– Expressing Adenoviral Vectors

We applied a Cre-loxP recombination system to generate adenoviral vectors for expressing FLAG-tagged soluble form TeM and ChM-I proteins, designated as f-sTeM and f-mChM-I, respectively. Because the backbone of the pALC3.0 cosmid vector was constructed by replacing the E1 region of the circular form of the adenoviral genome with the loxP-flanked cosmid cassette, cotransfection of a Cre-expression plasmid with the indicated pALC3.0 cosmid vector into 293 cells efficiently generates a recombinant adenoviral vector that contains the indicated expression cassette, but lacks the cosmid vector backbone. In our experiments, fluorescence microscopic examination revealed that in the presence of Cre recombinase, CPE appeared in all wells of the transfected 293 cells within 8 days of cultures. Because recombinant adenoviruses with a titer lower than 1×10^4 plaque-forming units (pfu)/cell did not cause apoptotic cell death in infected cells within 6 to 8 passages, infection of recombinant adenoviruses to culture cells for biological assay was performed at a multiplicity of infection (moi) of less than 2×10^3 pfu/cell to prevent cytotoxicity. In the present study, adenoviral vectors were designed to secrete the f-sTeM protein or the f-mChM-I protein through the secretion signal of preprotrypsin. Schematic structures of human TeM and the human ChM-I precursor and the construction maps for the indicated adenoviral vectors are shown in Figures 5A and 5B. The efficiency of adenoviral

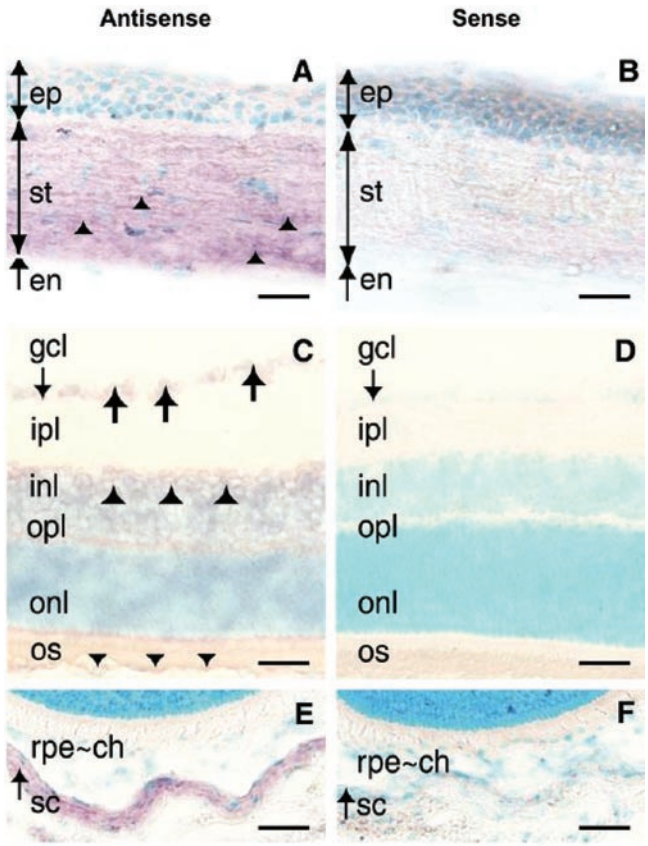

FIGURE 4. Expression of TeM mRNA in the eye of young adult mice. Serial sections of eyes of 4-week-old mice were hybridized with TeM antisense (**A**, **C**, **E**) or sense (**B**, **D**, **F**) riboprobes as a negative control. Positive signals of TeM mRNA were observed in the stromal layer of the cornea (**A**) and sclera (**E**). In the retina, positive signals were detected in the ganglion cell layer (**C**, *arrows*), inner nuclear layer (**C**, *large arrowheads*), and, faintly, in the RPE (**C**, *small arrowheads*). The sections were counterstained with methyl green. ep, epithelial cell layer; st, stromal layer; en, endothelial cell layer; gcl, ganglion cell layer; ipl, inner plexiform layer; inl, inner nuclear layer; opl, outer plexiform layer; onl, outer nuclear layer; os, outer segments; rpe, RPE; ch, choroidal layer; sc, sclera. Scale bars: (**A**, **B**) 250 μm; (**C**–**F**) 100 μm.

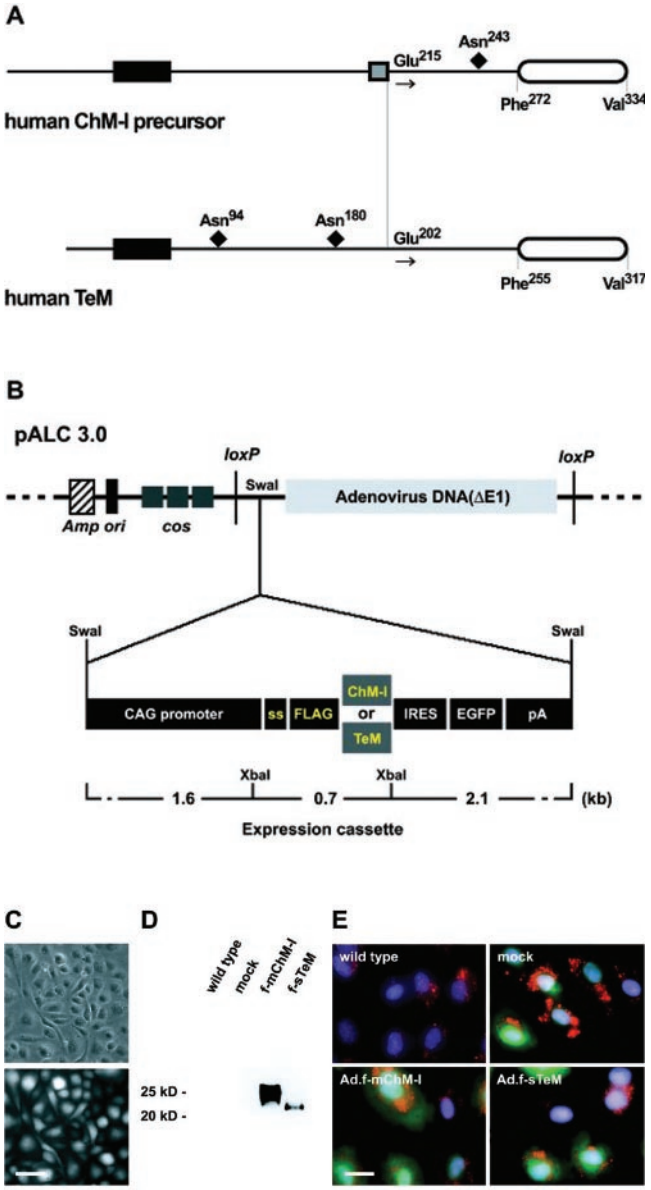

FIGURE 5. Adenoviral expression cassette construction and gene transduction of HRECs with adenoviral vectors. (**A**) Schematic structures of human TeM (GenBank Accession No. AF219993) and the human ChM-I precursor (AB006000). *Filled rectangles*: transmembrane domains. *Open ellipses*: the C-terminal cysteine-rich domains. *Gray box*: the processing signal (Arg^{211}-Glu-Arg-Arg^{214}) in the human ChM-I precursor. *Filled diamonds*: potential N-linked glycosylation sites. The C-terminal fragment (Glu^{202}-Val^{317}) of human TeM corresponds to the mature form (Glu^{215}-Val^{334}) of human ChM-I. (**B**) *Top*: structure of pALC3.0 cosmid vector with the indicated expression cassette. *Gray box*: 34-kb adenoviral genome. The cosmid vector backbone is flanked by *loxP* sites and includes three cos sites, the bacterial *ori*, and the ampicillin resistance gene (Ap). *Bottom*: structure of the f-mChM-I and f-sTeM expression cassettes. The expression cassette consists of the CAG promoter, the secretion signal of preprotrypsin (ss), the FLAG-tagged human TeM (Glu^{202}-Val^{317}) cDNA or the FLAG-tagged human ChM-I (Glu^{215}-Val^{334}) cDNA, and the IRES-EGFP cDNA, followed by a polyadenylation signal (pA). The expression cassette was inserted into the *Swa*I site of the cosmid vector. (**C**) *Top*: phase-contrast microscopic image of the cobblestone-like HRECs 24 hours after adenoviral gene transduction. *Bottom*: fluorescence microscopic image revealing efficient adenoviral gene transduction in HRECs. EGFP fluorescence was observed in almost 100% of the cells. (**D**) Western blot for f-sTeM and f-mChM-I with 15 μg protein from the conditioned medium of wild-type HRECs or HRECs transduced with the indicated adenoviral vectors. A broad band of ~25 kDa appeared in the lane of the conditioned medium, including f-mChM-I and a band of ~20 kDa in the lane of the conditioned medium, including f-sTeM. (**E**) Characterization of HREC cultures. Wild-type HRECs and the HRECs infected with the indicated adenoviral vectors were incubated with 10 μg/mL Dil-Ac-LDL in EGM2 medium for 6 hours and further incubated with 10 nM Hoechst 33342 for 2 hours. Digital images from the fluorescence microscope were merged on computer. *Green* fluorescence from EGFP marks the cells successfully transfected with adenovirus. Nuclei staining by Hoechst 33342 appears *blue-violet*. Dil-AcLDL uptake (*red*) was detectable in all the HRECs, regardless of adenoviral transduction. Scale bars: (**C**) 50 μm; (**E**) 20 μm.

transfection was monitored by the EGFP fluorescence. Almost 100% of the HRECs were successfully infected with the adenovirus (Fig. 5C). The EGFP fluorescence in the gene-transduced cells persisted for more than 1 week and gradually decreased in intensity with cell passages. Secretion of the f-sTeM protein or the f-mChM-I protein in the conditioned media was detected by Western blot with anti-FLAG monoclonal antibodies. A broad ~25-kDa immunoreactive band for the mature ChM-I (f-mChM-I) and a 21-kDa band for the soluble form TeM (f-sTeM) were detected in the indicated conditioned medium of HRECs, but not in the medium from the control cells (Fig. 5D). The differences in the protein amount and the molecular weight detected by Western blot enhanced the differences in glycosylation and solubility (hydrophobicity) between f-mChM-I and f-sTeM.

Preservation of the Endothelial Characteristics in HRECs after Adenoviral Infection

HRECs after adenoviral infection fulfilled the established criteria for identification of vascular endothelial cells—that is, they formed a monolayer with cobblestone morphology (Fig. 5C) and showed positive immunostaining for PECAM (data not shown) and the endothelial-cell–specific uptake of Dil-AcLDL. Almost 100% of the HRECs showed Dil-AcLDL, uptake both with and without adenoviral infection (Fig. 5E).

Suppression of HREC Proliferation by Autocrine Expression of the f-sTeM Protein or the f-mChM-I Protein

The suppressive effect of the f-sTeM protein and the f-mChM-I protein on VEGF-induced endothelial proliferation was evaluated by measurement of BrdU uptake. BrdU uptake in the wild-type HRECs and the HRECs infected with the empty adenoviral vector (mock) was significantly stimulated by VEGF in a dose-dependent manner, up to 30 ng/mL (Fig. 6A). In contrast, BrdU uptake in the HRECs transduced with the adenoviral vector, either for expressing the f-sTeM protein or for expressing the f-mChM-I protein, did not increase after the addition of VEGF (Fig. 6A). To further rule out the nonspecific cytoplasmic effects caused by the adenoviral infection, BrdU uptake of the HUVECs incubated with the conditioned media from the indicated adenoviral-vector–transduced HRECs was evaluated, and similar results were obtained (Fig. 6B).

Inhibition of Capillary Morphogenesis by Autocrine Expression of the f-sTeM Protein or the f-mChM-I Protein

To explore the in vitro antiangiogenic activity in the C-terminal domain of TeM, capillary-like morphogenesis of vascular endothelial cells on synthetic matrix (Matrigel; BD Labware) and in coculture with dermal fibroblasts were evaluated. Wild-type HRECs and the HRECs infected with the indicated adenoviral vectors were plated on the matrix in the presence of 10 ng/mL

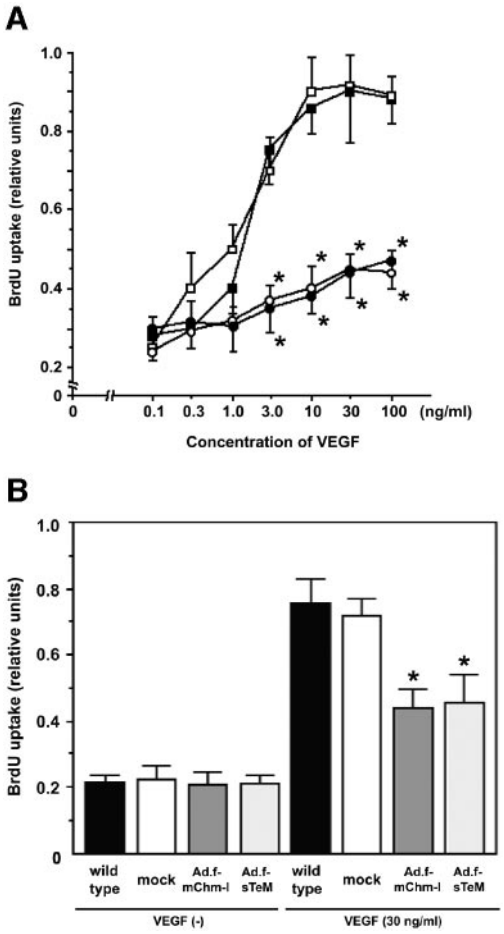

FIGURE 6. Inhibitory effect of constitutive f-sTeM or f-mChM-I expression on proliferation of HRECs and HUVECs. (**A**) HRECs were grown to subconfluence in a 96-well culture plate, starved in 0.5% FBS containing αMEM for 6 hours, and stimulated by 0.1, 0.3, 1, 3, 10, 30, and 100 ng/mL VEGF for 12 hours. DNA synthesis was evaluated as BrdU uptake by measurement of BrdU ELISA chemiluminescence. (□) Wild-type HRECs; (■) mock; (○) f-mChM-I–expressing HRECs; and (●) f-sTeM–expressing HRECs. Data are the mean ± SD of triplicate measurements. $^*P < 0.01$ versus wild-type HRECs. (**B**) HUVECs were grown to subconfluence in a 96-well culture plate, starved in 0.5% FBS-containing αMEM for 6 hours, and then cultured in a mixture of conditioned medium obtained from the indicated adenoviral gene–transduced HRECs and fresh DMEM at a ratio of 1:1. The cells were stimulated by 30 ng/mL VEGF for 12 hours, and DNA synthesis was evaluated by BrdU uptake measured using BrdU ELISA chemiluminescence. Data are the mean ± SD of triplicate measurements. $^*P < 0.01$ versus the HUVECs cultured in conditioned media from wild-type HRECs.

VEGF. Under these conditions, wild-type HRECs and mock cells aggregated and elongated to form capillary-like structures within a few hours (Fig. 7A). In contrast, there was a significant impairment of ability to elongate and to form capillary-like structures in the HRECs expressing f-sTeM or f-mChM-I. The total length of capillary-like structures per field in the adenovirus-transduced HRECs was significantly shorter than that of wild-type and that of mock transfectants (Fig. 7A, bottom).

To further confirm that the suppression of capillary-like formation is essentially attributable to the autocrine response of HRECs to the soluble TeM and ChM-I protein in the conditioned media, capillary formation of HUVECs was tested with the in vitro angiogenesis assay kit by culturing in various conditioned media. Capillary-like structures formed by HUVECs under the stimulation of VEGF were significantly inhibited by the conditioned media derived from f-sTeM and f-mChM-I overexpressing cells. In contrast, no inhibitory activities toward HUVEC capillary formation were observed in the condition medium from the wild-type cultured HRECs or from the mock cells (Fig. 7B).

DISCUSSION

Growth of new blood vessels is an important event pathologically and physiologically. During the embryonic stages, vasculogenesis and its regression are absolutely necessary for tissue and organ development, such as limb formation and lens development. Because vasculogenesis and its regression are also considered to be regulated and modulated by stimulatory and inhibitory factors, we investigated the expression pattern of TeM, a potent angiogenesis inhibitor, in mouse embryos and young adults. Northern blot analysis demonstrated that the TeM gene is expressed from the embryonic stage and in a tissue-specific manner. In contrast to the expression spike of ChM-I at embryonic day 7,[36] expression of TeM mRNA was initially noted from the late developmental phase of the embryo, a period of skeletal muscle development, suggesting the relationship between TeM gene expression and the formation of skeletal muscle. Other than the tendon and ligament, which are the major expression sites for TeM,[32,33] the eye and skin are newly noted as significant expression sites for TeM mRNA. The expression of both ChM-I and TeM in the eye and their predicted antiangiogenic functions lead us to speculate that ChM-I and TeM also function as antiangiogenic molecules in the eye. In a previous study, we have generated a polyclonal antibody against the human and mouse TeM protein sequence at amino acids 245-252 and successfully detected the recombinant TeM as a transmembrane type glycoprotein by means of cell surface biotinylation and immunoprecipitation.[31] In the current study, the expression of endogenous TeM protein in the eye was confirmed to be comparable with its mRNA distribution detected by Northern blot analysis. The molecular masses of ~40 kDa and ~45 kDa detected without any small bands for the endogenous TeM protein correspond well with the predicted molecular mass estimated from the full amino acid sequence, indicating that natural TeM protein in the eye may predominantly function as a transmembrane protein on the cell surface. The major band of ~40 kDa and the minor band of ~45 kDa are variant forms of TeM, due to different glycosylation in vivo.[31,32]

Although the presence of TeM mRNA in the eye has been suggested in previous studies,[31,33] the precise mRNA expression sites and the sites of protein expression have never been established. To further examine the site for expression and localization of TeM in the eye, RT-PCR, in situ hybridization, and immunohistochemistry were performed in mouse embryos and young adult mice. In the present study, TeM mRNA was detected in the tendon of the extraocular muscle and the sclerocornea, both of which are categorized as dense connective tissues, together with the tendon, ligament, and epimysium of skeletal muscles.[41] Other than these hypovascular connective tissues, significant TeM mRNA expression is notable in the lens epithelial cells at the equator and the early differentiating secondary lens fiber cells. The anterior cells of the lens vesicle generally proliferate and move toward the equator of the vesicle as lens development progresses. These cells eventually pass through the equatorial region to elongate.[42] It should be noted that the expression of TeM protein most abundantly in the differentiated secondary lens fibers just adjacent to the lens fiber cells that express TeM mRNA correlates well with the cell fate of differentiation in the lens fiber cells. However, TeM mRNA and its translated protein were no

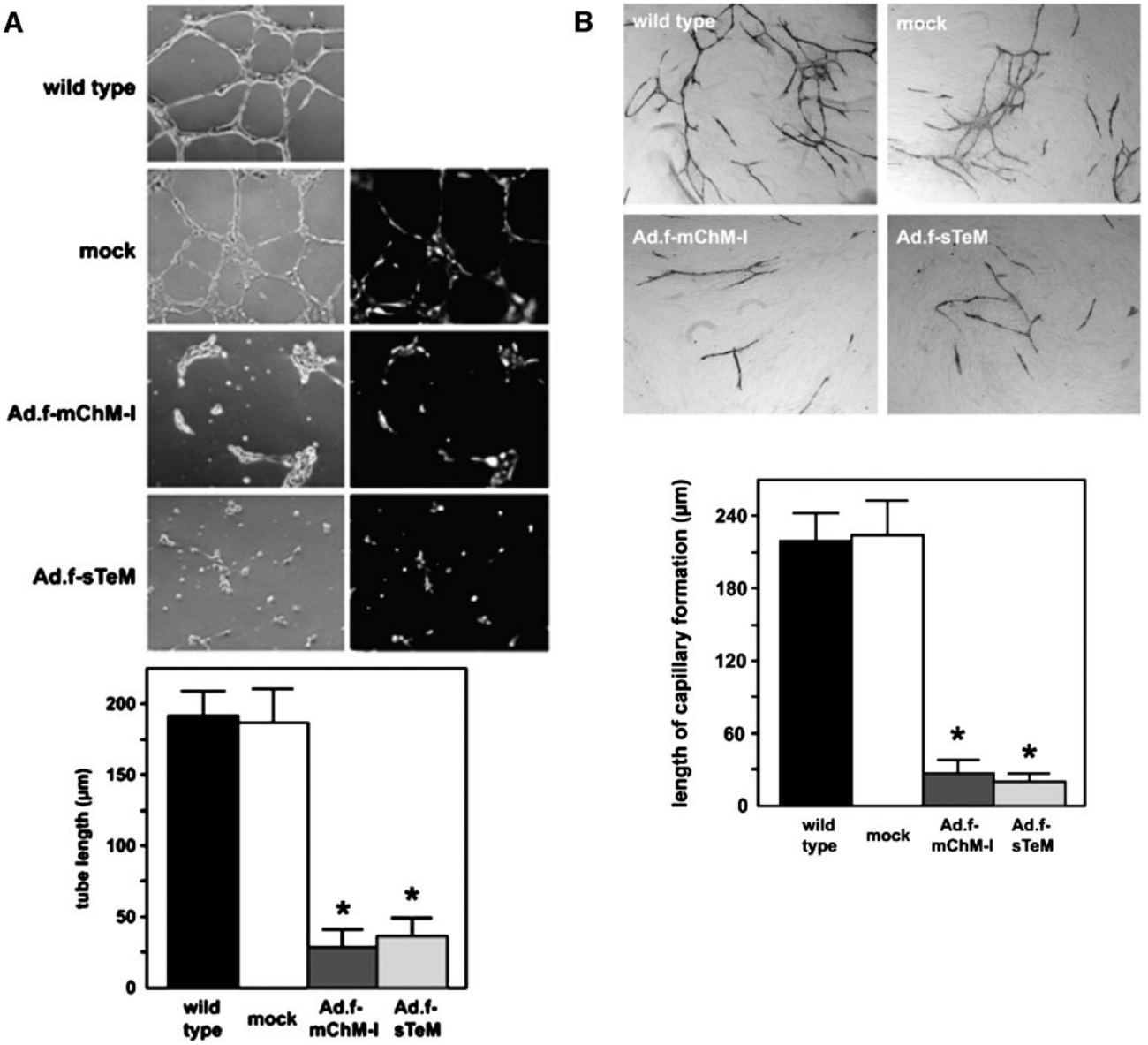

FIGURE 7. f-sTeM and f-mChM-I inhibited in vitro angiogenesis. (**A**) *Top*: representative phase-contrast (*left*) and fluorescence (*right*) micrographs show that cell aggregation and network formation were suppressed in HRECs transduced with the indicated adenoviral vector. The origin of fluorescence is the EGFP generated in the cells with the indicated adenoviral gene transduction. *Bottom*: Quantitative evaluation of the length of the capillary-like structures. Data are the mean ± SD of triplicate measurements. $^*P < 0.01$ versus wild-type HRECs. (**B**) *Top*: Representative phase-contrast micrographs of capillary structures formed by HUVECs. Cells were cocultured with human fibroblasts and incubated for 11 days with 10 ng/mL VEGF and the conditioned media from the indicated HREC cultures. *Bottom*: Quantitative evaluation of the length of the capillary structures by computer. Data are the mean ± SD of triplicate measurements. $^*P < 0.01$ versus HUVECs incubated in the conditioned medium from wild-type HRECs. Magnification: (**A**) ×150; (**B**) ×20.

longer expressed in any component of the lens from the neonatal stages together with the regression of the vascular networks surrounding the lens (data not shown). We also confirmed the disappearance of TeM expression in lens tissues by RT-PCR in 4-week-old mice. This spatiotemporal expression pattern led us to speculate that TeM in the lens fibers may function as antiangiogenic barriers for preventing vascular network growth into the lens itself during developmental stages of the lens and that expression is self-limited, responding to vascular regression.

In the developing retina, TeM mRNA and protein localization were detected in the inner neural retina and the RPE. As development progressed, TeM mRNA in the inner neural retina was found to be restricted to the ganglion cell layer and to the inner nuclear layer cells. In a previous analysis of adult rat eyes, we have shown that ChM-I mRNA is abundantly expressed in the nonpigment ciliary body, ganglion cell layer, and inner nuclear layer cells of the neural retina and the RPE.[28] Therefore, retina is concluded to be the major tissue where TeM and ChM-I are coexpressed. ChM-I proteins exist as a ~37-kDa precursor in its gene-expressing tissues and are then secreted into the aqueous humor and vitreous body as a ~25-kDa mature form through processing signals.[28] In contrast to ChM-I, we neither detected any processed form of TeM less than 40 kDa in the tissue extracts from whole eyes nor any positive immunohistochemical signals against TeM in aqueous humor and vitreous body. Together with the absence of processing signal throughout its amino acid sequence, TeM pro-

tein is thought to exist predominantly as the transmembrane form on the cell surface and not as the secreted form in the eyes. Because of the antiangiogenic characteristics included in the C terminus of TeM, expression of TeM during the late phase of embryogenesis may contribute to the angiostatic nature of lens and the restricted vascular formation in the retina.

Upregulation of VEGF in the aqueous humor and vitreous body has been shown to play an important role in intraocular angiogenesis, such as rubeotic glaucoma and the neovascular membrane proliferation observed in diabetic retinopathy.[6,43] In a physiological state, expression and localization of VEGF are detectable also in normal ocular vascularized tissues, such as the conjunctiva, iris, retina, and choroid-RPE complex.[13] These features strongly suggest the presence of antiangiogenic agents in the avascular parts of the eye, such as the sclerocornea, aqueous humor ,and vitreous body, for the prevention of vascular invasion. It is of interest that both ChM-I and PEDF are constitutively present in aqueous humor and vitreous body in a high concentration, possibly working to counterbalance the angiogenic stimulators.[21,28] As the cartilage and vitreous body where ChM-I is expressed is similar in hypovascularity and component (type II collagen),[44–47] so is the sclerocornea similar to the tendon and ligaments in the three-dimensional network of collagen fibers and hypovascularity categorized as dense connective tissues.[41,48,49] The cornea is a transparent avascular tissue. In physiological conditions, the vascular networks of the conjunctiva come close to the limbus and the corneoscleral junction, but never grow into the cornea itself. Sclera per se is also an avascular tissue consisting of the collagenous elastic fibers. Although large blood vessels, such as ciliary arteries penetrate the sclera and construct vascular networks in the chorioretinal layer, the vascular networks never divide within the sclera itself. These findings predict that the existence of angiogenesis inhibitors in the sclerocornea and TeM may be one of the candidates, supported by the revelation in the current study that the C-terminal fragment of TeM (Glu^{202}-Val^{317}) and ChM-I (Glu^{215}-Val^{334}) effectively inhibited in vitro angiogenesis. The existence of TeM as a transmembrane protein in the sclerocornea and the identification of its antiangiogenic domain on the cell surface may work as an antiangiogenic barrier for the physiological prevention of vascular invasion into these hypovascular tissues.

To the best of our knowledge, TeM and vascular endothelial growth inhibitor (VEGI), a novel member of the tumor necrosis factor family,[50] are the newly identified transmembrane-type angiogenesis inhibitors at present. The antiangiogenic functional region in VEGI was found to be downstream of the transmembrane domain, possibly functioning between the cell–cell or cell–matrix interfaces. Local production of the secreted form VEGI through gene transfer has been reported to suppress tumor growth through the complete arrest of angiogenesis.[50,51] As we have shown in the present study, the C-terminal fragments (i.e., Glu^{202}-Val^{317} and Glu^{215}-Val^{334}) of TeM and ChM-I, both of which are located downstream of the transmembrane domain, are responsible for their antiangiogenic activity. Significant suppression of cell proliferation and in vitro angiogenesis were observed in the HRECs by adenoviral gene transduction. The conditioned media from soluble TeM (Glu^{202}-Val^{317})– or ChM-I (Glu^{215}-Val^{334})–expressing cells also showed a marked inhibitory effect on in vitro angiogenesis of HUVECs. These results also offer the therapeutic possibility for the management of intraocular angiogenesis by gene transduction of TeM and/or ChM-I in vivo. The in vivo study with hypoxia model is now under way.

In summary, we elucidated in the current study the expression and localization pattern of TeM, a transmembrane-type ChM-I–related protein, in mouse eyes and explored the antiangiogenic characteristics in the C-terminal region of TeM by generating a recombinant secreted isoform. Further investigations are needed to clarify fully the mechanism of both TeM and ChM-I for the inhibition of angiogenesis and the safety of using these molecules in clinical applications.

References

1. Adamis AP, Aiello LP, D'Amato RA. Angiogenesis and ophthalmic disease. *Angiogenesis.* 1999;3:9–14.
2. Aiello LP. Keeping in touch with angiogenesis. *Nat Med.* 2000;6:379–381.
3. Folkman J, Klagsberun M. Angiogenic factor. *Science.* 1987;235:442–447.
4. Glaser BM. Extracellular modulating factors and the control of intraocular neovascularization. *Arch Ophthalmol.* 1990;160:603–607.
5. Yoshida A, Yoshida S, Khalil AK, Ishibashi T, Inomata H. Role of NF-kappaB-mediated interleukin-8 expression in intraocular neovascularization. *Invest Ophthalmol Vis Sci.* 1998;39:1097–1106.
6. Aiello LP, Avery RL, Arrigg PG, et al. Vascular endothelial growth factor in ocular fluid of patients with diabetic retinopathy and other retinal disorders. *N Engl J Med.* 1994;331:1480–1487.
7. Pierce EA, Avery RL, Foley ED, Aiello LP, Smith LE. Vascular endothelial growth factor/vascular permeability factor expression in a mouse model of retinal neovascularization. *Proc Natl Acad Sci USA.* 1995;92:905–909.
8. Ogata N, Tombran-Tink J, Nishikawa M, et al. Pigment epithelium-derived factor in the vitreous is low in diabetic retinopathy and high in rhegmatogenous retinal detachment. *Am J Ophthalmol.* 2001;132:378–382.
9. Schweigerer L, Malerstein B, Neufeld G, Gospodarowicz D. Basic fibroblast growth factor is synthesized in cultured retinal pigment epithelial cells. *Biochem Biophys Res Commun.* 1987;143:934–940.
10. Sivalingam A, Kenney J, Brown GC, Benson WE, Donoso L. Basic fibroblast growth factor levels in the vitreous of patients with proliferative diabetic retinopathy. *Arch Ophthalmol.* 1990;108:869–872.
11. Meyer-Schwickerath R, Pfeiffer A, Blum WF, et al. Vitreous levels of the insulin-like growth factors I and II, and the insulin-like growth factor binding proteins 2 and 3, increase in neovascular eye disease: studies in nondiabetic and diabetic subjects. *J Clin Invest.* 1993;92:2620–2625.
12. Gerhardinger C, Brown LF, Roy S, Mizutani M, Zucker CL, Lorenzi M. Expression of vascular endothelial growth factor in the human retina and in nonproliferative diabetic retinopathy. *Am J Pathol.* 1998;152:1453–1462.
13. Kim I, Ryan AM, Rohan R, et al. Constitutive expression of VEGF, VEGFR-1, and VEGFR-2 in normal eyes. *Invest Ophthalmol Vis Sci.* 1999;40:2115–2121.
14. Glaser BM, Campochiaro PA, Davis JL Jr, Sato M. Retinal pigment epithelial cells release an inhibitor of neovascularization. *Arch Ophthalmol.* 1985;103:1870–1875.
15. Brem S, Brem H, Folkman J, Finkelstein D, Patz A. Prolonged tumor dormancy by prevention of neovascularization in the vitreous. *Cancer Res.* 1976;36:2807–2812.
16. Lutty GA, Thompson DC, Gallup JY, Mello RJ, Patz A, Fenselau A. Vitreous: an inhibitor of retinal extract-induced neovascularization. *Invest Ophthalmol Vis Sci.* 1983;24:52–56.
17. Jacobson B, Basu PK, Hasany SM. Vascular endothelial cell growth inhibitor of normal and pathologic human vitreous. *Arch Ophthalmol.* 1984;102:1543–1545.
18. Jacobson B, Dorfman T, Basu PK, Hasany SM. Inhibition of vascular endothelial cell growth and trypsin activity by vitreous. *Exp Eye Res.* 1985;41:581–595.
19. Lutty GA, Mello RJ, Chandler C, Fait C, Bennett A, Patz A. Regulation of cell growth by vitreous humour. *J Cell Sci.* 1985;76:53–65.
20. Williams GA, Eisenstein R, Schumacher B, Hsiao KC, Grant D. Inhibitor of vascular endothelial cell growth in the lens. *Am J Ophthalmol.* 1984;97:366–371.

21. Dawson DW, Volpert OV, Gillis P, et al. Pigment epithelium-derived factor: a potent inhibitor of angiogenesis. *Science.* 1999; 285:245–248.
22. Duh EJ, Yang HS, Suzuma I, et al. Pigment epithelium-derived factor suppresses ischemia-induced retinal neovascularization and VEGF-induced migration and growth. *Invest Ophthalmol Vis Sci.* 2002;43:821–829.
23. Ogata N, Wada M, Otsuji T, Jo N, Tombran-Tink J, Matsumura M. Expression of pigment epithelium-derived factor in normal adult rat eye and experimental choroidal neovascularization. *Invest Ophthalmol Vis Sci.* 2002;43:1168–1175.
24. Hiraki Y, Tanaka H, Inoue H, Kondo J, Kamizono A, Suzuki F. Molecular cloning of a new class of cartilage-specific matrix, chondromodulin-I, which stimulates growth of cultured chondrocytes. *Biochem Biophys Res Commun.* 1991;175:971–977.
25. Hiraki Y, Inoue H, Iyama K, et al. Identification of chondromodulin I as a novel endothelial cell growth inhibitor: purification and its localization in the avascular zone of epiphyseal cartilage. *J Biol Chem.* 1997;272:32419–32426.
26. Hiraki Y, Kono T, Sato M, Shukunami C, Kondo J. Inhibition of DNA synthesis and tube morphogenesis of cultured vascular endothelial cells by chondromodulin-I. *FEBS Lett.* 1997;415:321–324.
27. Dietz UH, Ziegelmeier G, Bittner K, Bruckner P, Balling R. Spatiotemporal distribution of chondromodulin-I mRNA in the chicken embryo: expression during cartilage development and formation of the heart and eye. *Dev Dyn.* 1999;216:233–243.
28. Funaki H, Sawaguchi S, Yaoeda K, et al. Expression and localization of angiogenesis inhibitory factor, chondromodulin-I, in adult rat eye. *Invest Ophthalmol Vis Sci.* 2001;42:1193–1200.
29. Hiraki Y, Mitsui K, Endo N, et al. Molecular cloning of human chondromodulin-I, a cartilage-derived growth modulating factor, and its expression in Chinese hamster ovary cells. *Eur J Biochem.* 1999;260:869–878.
30. Hayami T, Shukunami C, Mitsui K, et al. Specific loss of chondromodulin-I gene expression in chondrosarcoma and the suppression of tumor angiogenesis and growth by its recombinant protein in vivo. *FEBS Lett.* 1999;458:436–440.
31. Yamana K, Wada H, Takahashi Y, Sato H, Kasahara Y, Kiyoki M. Molecular cloning and characterization of CHM1L, a novel membrane molecule similar to chondromodulin-I. *Biochem Biophys Res Commun.* 2001;280:1101–1106.
32. Shukunami C, Oshima Y, Hiraki Y. Molecular cloning of tenomodulin, a novel chondromodulin-I related gene. *Biochem Biophys Res Commun.* 2001;280:1323–1327.
33. Brandau O, Meindl A, Fassler R, Aszodi A. A novel gene, tendin, is strongly expressed in tendons and ligaments and shows high homology with chondromodulin-I. *Dev Dyn.* 2001;221:72–80.
34. Graham FL, Smiley J, Russell WC, Nairn R. Characteristics of a human cell line transformed by DNA from human adenovirus type 5. *J Gen Virol.* 1977;36:59–74.
35. Chomczynski P, Sacchi N. Single-step method of RNA isolation by acid guanidinium thiocyanate-phenol-chloroform extraction. *Anal Biochem.* 1987;162:156–159.
36. Shukunami C, Iyama K, Inoue H, Hiraki Y. Spatiotemporal pattern of the mouse chondromodulin-I gene expression and its regulatory role in vascular invasion into cartilage during endochondral bone formation. *Int J Dev Biol.* 1999;43:39–49.
37. Niwa H, Yamamura K, Miyazaki J. Efficient selection for high-expression transfectants with a novel eukaryotic vector. *Gene.* 1991;108:193–199.
38. Tashiro F, Niwa H, Miyazaki J. Constructing adenoviral vectors by using the circular form of the adenoviral genome cloned in a cosmid and the Cre-loxP recombination system. *Hum Gene Ther.* 1999;10:1845–1852.
39. Miyake S, Makimura M, Kanegae Y, et al. Efficient generation of recombinant adenoviruses using adenovirus DNA-terminal protein complex and a cosmid bearing the full-length virus genome. *Proc Natl Acad Sci USA.* 1996;93:1320–1324.
40. Bishop ET, Bell GT, Bloor S, Broom IJ, Hendry NFK, Wheatley DN. An in vitro model of angiogenesis: basic features. *Angiogenesis.* 1999;3:335–344.
41. Young B, Heath J. Connective tissues. In: Burkitt H, et al., eds., *Wheaters Functional Histology.* Edinburgh, Scotland, UK: Churchill Livingstone; 2000;97–192.
42. Goldberg MF. Persistent fetal vasculature (PFV): an integrated interpretation of signs and symptoms associated with persistent hyperplastic primary vitreous (PHPV). LIV Edward Jackson Memorial Lecture. *Am J Ophthalmol.* 1997;124:587–626.
43. Miller JW, Adamis AP, Aiello LP. Vascular endothelial growth factor in ocular neovascularization and proliferative diabetic retinopathy. *Diabetes Metab Rev.* 1997;13:37–50.
44. Snowden JM, Swann DA. Vitreous structure. V. The morphology and thermal stability of vitreous collagen fibers and comparison to articular cartilage (type II) collagen. *Invest Ophthalmol Vis Sci.* 1980;19:610–618.
45. Liang JN, Chakrabarti B. Spectroscopic studies on pepsin-solubilized vitreous and cartilage collagens. *Curr Eye Res.* 1981;1:175–181.
46. Poole AR, Pidoux I, Reiner A, Coster L, Hassell JR. Mammalian eyes and associated tissues contain molecules that are immunologically related to cartilage proteoglycan and link protein. *J Cell Biol.* 1982;93:910–920.
47. Nguyen BQ, Fife RS. Vitreous contains a cartilage-related protein. *Exp Eye Res.* 1986;43:375–382.
48. Snowden JM, Eyre DR, Swann DA. Vitreous structure. VI. Age-related changes in the thermal stability and crosslinks of vitreous, articular cartilage and tendon collagens. *Biochim Biophys Acta.* 1982;706:153–157.
49. Heinegard D, Bjorne-Persson A, Coster L, et al. The core proteins of large and small interstitial proteoglycans from various connective tissues form distinct subgroups. *Biochem J.* 1985;230:181–194.
50. Zhai Y, Ni J, Jiang GW, et al. VEGI, a novel cytokine of the tumor necrosis factor family, is an angiogenesis inhibitor that suppresses the growth of colon carcinomas in vivo. *FASEB J.* 1999;13:181–189.
51. Zhai Y, Yu J, Iruela-Arispe L, et al. Inhibition of angiogenesis and breast cancer xenograft tumor growth by VEGI, a novel cytokine of the TNF superfamily. *Int J Cancer.* 1999;82:131–136.